

Quantitative Analysis of Reaction Front Geometry in Detonations

F. Pintgen and J.E. Shepherd
Graduate Aeronautical Laboratories
California Institute of Technology
Pasadena, California 91125

*Submitted to the International Colloquium on Application of Detonation for Propulsion,
St. Petersburg, Russia, July 6-9, 2004.*

Previous observations (Pintgen et al., 2003b, Pintgen, 2000) on the reaction zone structure of propagating detonations show that mixtures with very regular cellular patterns have smooth reaction fronts as visualized by Planar Laser Induced Fluorescence (PLIF) images of the OH radical. Mixtures with more irregular cellular structure exhibit (Pintgen et al., 2003a, Austin, 2003) shear flow instabilities and fine-scale wrinkling of the reaction front. From the PLIF and Schlieren images, the reaction front appears to be quite geometrically complex in the case of irregular cellular structure. The extent of geometric complexity is an important issue (Singh et al., 2003) in determining the relative roles of chemical reaction due to chain-branching thermal explosion associated with shock compression as compared to diffusive transport from the hotter into the cooler regions.

In the present paper, we carry out quantitative analyses of the reaction front geometry complexity by analyzing the PLIF images and imaging system. The front geometry is characterized by examining two characteristics: the rectified length and the effective dimension. The geometric and the stability characteristics of the mixtures are correlated using as a figure of merit the reduced effective activation energy as computed from detailed chemical reaction mechanisms. The mixtures studied vary in the degree of cellular regularity from “regular” to “highly irregular”, corresponding to effective reduced activation energies θ between 5.2 and 12.4.

The experiments were carried out in an 8-m long detonation tube attached to a 150×150 mm square test section, described in more detail in Pintgen et al. (2003b). The detonation velocities are obtained from six pressure transducers, three of which are in the test section, and are within 5% of the Chapman-Jouguet (CJ) value. PLIF imaging of the OH radical is used to visualize the reaction front through a 150-mm diameter quartz window in the side wall of the test section. The PLIF system is based on an excimer-pumped dye laser creating a light sheet with a 284.008 nm wavelength and imaging the fluorescence with an intensified charge-coupled device camera (ICCD) as described in Pintgen et al. (2003b) and in more detail in Pintgen (2000).

Stoichiometric $\text{H}_2\text{-O}_2$ and $\text{H}_2\text{-N}_2\text{O}$ mixtures diluted with Ar or N_2 at initial conditions of 20 kPa and 20°C were investigated and data from a total of 68 shots were analyzed. One PLIF image is obtained from each experiment. The distinct OH concentration front seen in all PLIF images indicates the location of the sharp rise in the OH concentration at the end of the induction zone as discussed in Pintgen et al. (2003b). The exponential rise in OH concentration coincides approximately with the sharpest temperature increase as seen in calculated OH profiles. In the present study, we will refer to the leading edge of the OH fluorescence front simply as the “reaction front”.

The computed reaction zone length (using detailed chemical kinetics mechanisms) at CJ conditions for the mixtures studied varies from 0.8 to 7.5 mm. The reduced activation energy $\theta = E_a/RT_{vN}$ was calculated by numerically evaluating the logarithmic derivative of the induction time t_i with respect to the postshock temperature. The cell sizes ranged from 22 to 110 mm as measured with soot foils placed on the side wall of the test section. It was difficult to assign a cell size S for the marginal mixtures, $S \geq 80$ mm, since a whole range of cell sizes was present. For these cases, the largest cell size observed on the soot foils is given. The $\text{H}_2\text{-O}_2\text{-Ar}$ mixture represents a mixture with a very regular cellular structure, $\theta = 5.2\text{-}5.6$. The $\text{N}_2\text{-diluted H}_2\text{-O}_2$ mixture is an example of a more irregular mixture, $\theta = 6.8\text{-}8.8$; whereas the $\text{H}_2\text{-N}_2\text{O}$ mixture diluted with N_2 is highly irregular, $\theta = 11.5\text{-}12.4$.

The reaction fronts were obtained by image processing. Examples of the results are shown in Fig. 1. It is obvious from visual examination of these images that the reaction fronts of mixtures classified as “irregular” have a much greater geometric complexity than those of the “regular” mixtures. However, to go beyond this simple observation and make a quantitative analysis of the reaction front geometry requires an evaluation of the imaging system qualities. The key issues are motion blur, modulation transfer function (MTF), light sheet thickness, and image processing.

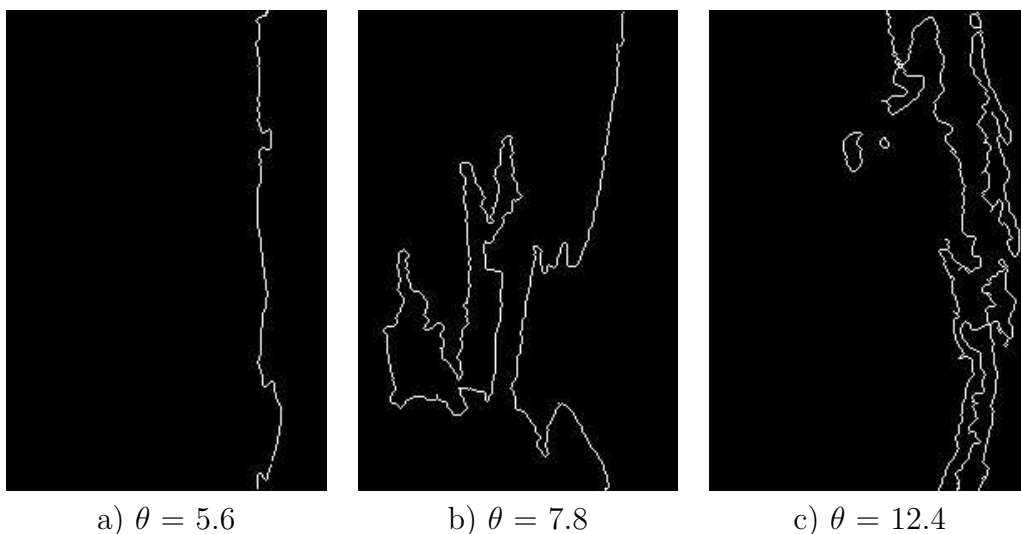


Figure 1: Three examples of edge-detected PLIF images. a) Shot 1653, $2\text{H}_2+\text{O}_2+17\text{Ar}$, image height: 40 mm, cell size: 47 mm; b) Shot 1619, $2\text{H}_2+\text{O}_2+6\text{N}_2$, image height: 30 mm, largest cell size observed on soot foil 80 mm; c) Shot 1591, $\text{H}_2+\text{N}_2\text{O}+3\text{N}_2$, image height 30 mm, largest cell size observed on soot foil: 120 mm

The conclusion from considering all of these effects is that the resolution is not limited by the digital nature of the ICCD but rather by the illumination technique and the degradation of the image due to the contrast reduction resulting from the other optical components, the lens and intensifier. The smallest scale resolvable depends on the image height and ranges from 0.7 to 1.2 mm for images between 30 to 70 mm high. This estimate is based on summing the separate influences of the MTF, light sheet thickness, and motion blur. The MTF was only measured for $m = 0.28$ and approximated as constant for the range

of magnifications used. The quoted resolution is in terms of actual physical dimensions of the object. We conclude that we can resolve features that are, in the best cases, one order of magnitude smaller than the ZND-CJ reaction zone length and two orders of magnitude smaller than the cell size. In the worst cases, the resolution is comparable to the ZND-CJ reaction zone length. Fortuitously, the resolution is best for the irregular cases where we are most interested in resolving the largest range of scales possible.

The two-dimensional slices of the reaction fronts have been characterized by using two measures of geometric complexity. First, we have used an approximate integration method to find the total edge length normalized by the image height. Second, we have used the box-counting method of fractal analysis to determine an average dimension of the fronts.

The normalized edge lengths measured for the “regular” mixtures (Ar-diluted H₂-O₂) ranges from the minimum of 1 up to 1.8, small compared to the other mixtures studied. For higher reduced activation energies θ , the maximum normalized edge length and range is increasing and reaches, for mixtures with $\theta \approx 8$, values up to 4.2. The minimum normalized edge length appears independent of θ and close to 1. For the “highly irregular” mixtures studies with $\theta = 12.4$, values up to 7.5 are measured.

A dimension, Fig. 2b, was found for each image using a linear least-squares fit to determine D by approximating the box coverage count N as a function of scale length λ

$$\log(N) = -D \log(\lambda/\lambda_0) + \text{constant} \quad (1)$$

for the range $-1.9 \leq \log(\lambda/\lambda_0) \leq -0.5$, corresponding to box sizes from 4×4 to 96×96 pixel where λ_0 is the height of the image..

As for the normalized edge length, a range of dimensions is obtained for each θ . For $\theta \leq 6$, the spread is small and the dimensions range from 1.05 up to 1.15. For intermediate values of θ , the dimensions range between 1.05 and 1.4 and, for the highest value of $\theta = 12.4$, the maximum dimension of 1.5 is obtained. The larger maximum values of the dimensions obtained for higher values of θ are quantitative evidence for the increasing degree of corrugation of the reaction front for higher values of θ .

The key limitation of this and all other techniques based on light sheet illumination is the lack of out-of-plane information. Due to the high-speed nature of flow and the apparatus we are using, we are also unable to obtain more than one realization per experiment. Based on our experience (Pintgen et al., 2003b) with more regular mixtures, we can identify several effects these limitations can mask and lead to misconceptions when interpreting these images. These include the uncontrolled orientation of the cellular structure to the light sheet and random variations in the phasing of the transverse waves. Despite these issues in interpretation, it is clear from inspecting Fig. 2 that, for the irregular mixtures, the effective reaction front transverse length is at least one order of magnitude larger than for the regular mixtures. Further work is needed in order to extend the present results from the image slices to the entire reaction front. This step is needed in order to connect the geometric analysis to the physical processes of combustion and address the question of the role of diffusion in highly irregular detonation fronts.

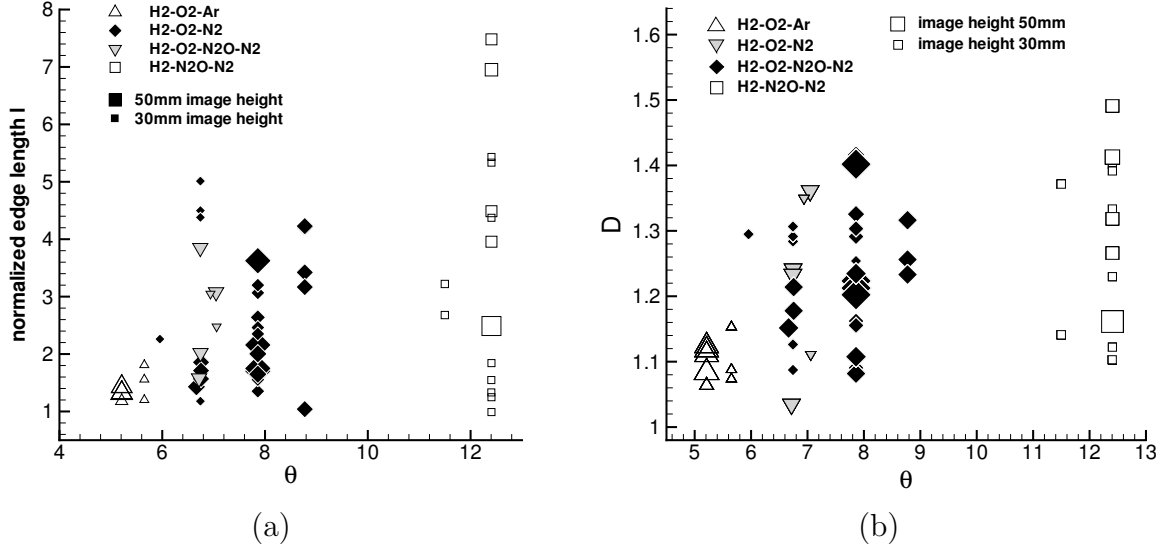


Figure 2: (a) Total edge length as a function of the reduced activation energy θ . (b) Dimension obtained from least-squares linear fit as a function of the reduced activation energy θ . Symbol size scales with height of field of view.

Acknowledgments

This work was supported by Stanford University Contract PY-1905 under Dept. of Navy Grant No. N00014-02-1-0589 “Pulse Detonation Engines: Initiation, Propagation, and Performance”.

References

- Joanna Austin. *The Role of Instability in Gaseous Detonation*. PhD thesis, California Institute of Technology, Pasadena, California, June 2003.
- F. Pintgen, J. M. Austin, and J. E. Shepherd. Detonation front structure: Variety and characterization. In G.D. Roy, S.M. Frolov, R.J. Santoro, and S.A. Tsyganov, editors, *Confined Detonations and Pulse Detonation Engines*, pages 105–116. Torus Press, Moscow, 2003a.
- F. Pintgen, CA Eckert, JM Austin, and JE Shepherd. Direct observations of reaction zone structure in propagating detonations. *Combustion and Flame*, 133(3):211–229, 2003b.
- Florian Pintgen. *Laser-Optical Visualization of Detonation Structures*. Diplomarbeit, Lehrstuhl für Thermodynamik: Technische Universität München / Graduate Aeronautical Laboratories: California Institute of Technology, Munich, Germany, December 2000.
- S. Singh, D. Lieberman, and J. E. Shepherd. Combustion behind shock waves. Paper 03F-29 Western States Section/Combustion Institute, October 2003.